

This article was downloaded by:

On: 14 January 2011

Access details: *Access Details: Free Access*

Publisher *Taylor & Francis*

Informa Ltd Registered in England and Wales Registered Number: 1072954 Registered office: Mortimer House, 37-41 Mortimer Street, London W1T 3JH, UK



Molecular Simulation

Publication details, including instructions for authors and subscription information:

<http://www.informaworld.com/smpp/title~content=t713644482>

Molecular simulation of realistic membrane models of alkylated PEEK membranes

E. Tocci^a; P. Pullumbi^b

^a Research Institute for Membrane Technology ITM-CNR, c/o Università della Calabria, Rende (CS), Italy ^b Air Liquide, Centre de Recherche Claude-Delorme, Jouy-en-Josas Cedex, France

To cite this Article Tocci, E. and Pullumbi, P.(2006) 'Molecular simulation of realistic membrane models of alkylated PEEK membranes', *Molecular Simulation*, 32: 2, 145 — 154

To link to this Article: DOI: 10.1080/08927020600654645

URL: <http://dx.doi.org/10.1080/08927020600654645>

PLEASE SCROLL DOWN FOR ARTICLE

Full terms and conditions of use: <http://www.informaworld.com/terms-and-conditions-of-access.pdf>

This article may be used for research, teaching and private study purposes. Any substantial or systematic reproduction, re-distribution, re-selling, loan or sub-licensing, systematic supply or distribution in any form to anyone is expressly forbidden.

The publisher does not give any warranty express or implied or make any representation that the contents will be complete or accurate or up to date. The accuracy of any instructions, formulae and drug doses should be independently verified with primary sources. The publisher shall not be liable for any loss, actions, claims, proceedings, demand or costs or damages whatsoever or howsoever caused arising directly or indirectly in connection with or arising out of the use of this material.

Molecular simulation of realistic membrane models of alkylated PEEK membranes

E. TOCCI† and P. PULLUMBI‡*

†Research Institute for Membrane Technology ITM-CNR, c/o Università della Calabria, Via P. Bucci, Cubo 17/C, I-87030 Rende (CS), Italy

‡Air Liquide, Centre de Recherche Claude-Delorme, B. P. 126, Les-Loges-en-Josas, 78354 Jouy-en-Josas Cedex, France

(Received November 2005; in final form February 2006)

Atomistic molecular modelling has proven to be a useful tool for the investigation of transport properties of small gas molecules in polymer membrane matrices. The quality of the predictions of these properties based on molecular simulation depends principally on the quality of the membrane model. The predicted gas transport properties of small gas molecules in the same glassy polymer membrane show often a large scatter in gas diffusion and solubility simulated values. In order to reduce the scatter in predicted gas transport properties in glassy polymer membranes, numerical analysis of structural features of the membrane model is used for pre-selecting only the realistic ones for further simulations using transition-state theory (TST) approach. Simulation results of gas solubility and diffusion in alkylated poly-ether-ether-ketone (PEEK) membranes will illustrate the approach.

Keywords: Glassy polymer membrane; Molecular simulation; Solubility; Diffusion; Permeability; Small gas molecules

1. Introduction

Transport properties of small molecules in amorphous polymer matrices play an important role in many industrial applications such as gas separation of mixtures, packaging applications ranging from food conservation to controlled drug and cosmetics release, to special coatings for protecting specific substrates from gases. The prediction of transport properties of small molecules through polymer matrices would allow for the rational selection of polymer materials used in these applications and their future optimal design. Although there has been reported an increasing number of studies on this subject over the last decades [1–20], the prediction of transport properties of gas molecules through glassy polymer membranes remains a difficult target. In many of the recent studies, reporting molecular simulation prediction of diffusion and solubility of small gas molecules in several membrane models of the same glassy polymer a great scatter of the predicted values is observed. These results clearly indicate that the quality of the packing of the polymer chain into an amorphous cell membrane model strongly impacts the predicted gas transport properties.

The potential application of a polymer as a separation membrane depends upon the possible throughput and the purity of product [21–23]. This means that both the permeability of the gas that is transported more rapidly and the selectivity should be as large as possible. The permeability coefficient P of a small molecule through a polymer membrane is defined as the product of the diffusion coefficient D (kinetic parameter) and of the solubility coefficient S (thermodynamic parameter). The estimation of these coefficients can be done, either by molecular dynamics (MD) and Grand Canonical Monte Carlo (GCMC) simulations, or by applying the TST method provided that the quality of the membrane amorphous cells used in the calculation represent the real distribution of torsion angles, of the free volume and its distribution, as well as, the structural, conformational and volumetric properties of polymer membranes. The selectivity of a polymer membrane for a pair (i, j) of gas molecules is characterized by the ideal separation factor α_{ij} defined in equation (1):

$$\alpha_{ij} = \frac{P_i}{P_j} = \frac{S_i D_i}{S_j D_j} \quad (1)$$

*Corresponding author. E-mail: p.pullumbi@airliquide.com

Following this definition the selectivity of a membrane is the product of solubility selectivity (S_i/S_j) and diffusion selectivity (D_i/D_j). In the case of glassy polymer membranes the overall selectivity is mainly controlled by diffusion selectivity.

In the past 21 years, the control of gas permeability and permselectivity of polymer membranes has become a subject of strong research with worldwide participation in both industrial and academic laboratories [22,24–27]. To achieve such control, it has been necessary to reach a good understanding of the relationship between the properties of the polymers and their gas transport properties. However, it has been found that simple structural modifications, which lead to increase in polymer permeability usually, cause loss in permselectivity and *vice versa*. This so-called “trade-off” relationship has been well described in the literature [21,24,25,28,29]. The upper bound limit is not fixed in the α - P space but moves with time as new polymers with optimised structures become available.

Recent studies, indicate that in addition to the free volume content, gas transport parameters depend upon the backbone chain rigidity, its segmental mobility, the inter-chain distance and the chain interactions. For example, the introduction of bulky alkyl substituents opens up the polymer matrix resulting in a greater permeability. Also the reported introduction of *n*-alkyl side groups on a polymer backbone increases the side-chain flexibility as well as the membrane free volume with an overall increase of the permeability [21,22,30–32].

Modified poly-ether-ether-ketone (PEEK-WC) [33,34] are of considerable interest due to their excellent mechanical toughness, thermo-oxidative stability, solvent resistance and high transition temperature. In addition PEEK-WC, in contrast to the traditional crystalline PEEK, is soluble in a wide range of solvents and can be cast into flexible tough films [35–38]. In the last decade, considerable effort has been spent to introduce chemical modifications in this class of polymers in order to obtain better physical properties and to build-up membranes for electro dialysis, gas dehumidification and gas separation. Relatively few atomistic simulations have been performed on this class of polymers [14,39,40], since generating an appropriate equilibrium conformation is more computationally challenging than with an atactic polyolefins [41].

The purpose of the molecular simulations performed in this study is to demonstrate the importance of realistic representation of structural features of glassy polymer membranes models for predicting gas transport properties using the MD technique. A methodology for generating realistic models of membranes will be used for finding a relationship between chemical structure and conformational properties of alkylated PEEKs and gas permeabilities through them. Details of simulated self-diffusion, solubility and structural properties will be reported for the unsubstituted PEEK and for three synthesized alkylated PEEKs [42], namely dimethyl PEEK-WC (DMPEEK), tetramethyl PEEK-WC (TMPEEK) and diisopropyl

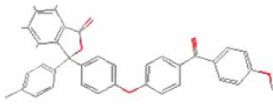
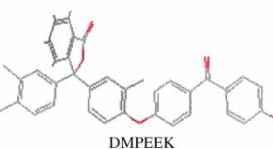
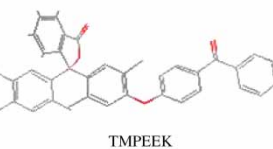
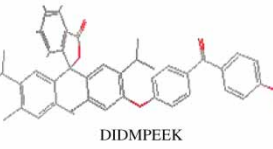
Monomer Structure	ρ (g cm ⁻³)	T_g (K)
 PEEK-WC	1.25	501
 DMPEEK	1.247	512
 TMPEEK	1.195	519
 DIDMPEEK	1.140	514

Figure 1. Monomer structures and experimental data of selected PEEKs.

dimethyl PEEK WC (DIDMPEEK). The monomer structure, experimental density and the glass transition temperature of the four PEEK is reported in figure 1.

2. Computational method

The estimation of the diffusion coefficient D , of the solubility coefficient S (and consequently of permeability P) of small per-meant molecules in a polymeric membrane is strongly dependent on the quality of the amorphous cell used in the calculation. This is particularly true in the case of stiff chain polymers containing aromatic moieties. In this study several amorphous packing of the polymer chain for the four PEEKs, reported in figure 1, followed by model equilibration and prediction of gas transport properties, have been carried out using the InsightII (400P+) molecular modelling package [43] for materials sciences together with condensed-phase optimized molecular potentials for atomistic simulation studies (COMPASS) force field [44,45] on two SGI octane machines.

For each of the PEEK polymer three independent atomistic bulk models were generated. The cubic basic volume element first has been filled with segments of a growing chain under periodic boundary conditions following a combination of the Theodorou–Suter [41] chain-generation approach and the Meirovitch's scanning method [46] reproducing the natural distribution of conformation

angles. In the case of polymers without aromatic moieties the size of the volume element can be chosen so as to reproduce the experimentally observed or theoretically predicted macroscopic density of the relevant polymer. For partly aromatic polymers, however, the chain packing stage has to be performed at very low densities to avoid ring-catenation. We have inserted “solvent” molecules in the initial phase of amorphous cell construction in order to avoid ring-catenation. Different multistage equilibration procedures after sequential removal of “solvent” molecules followed by energy minimisation and MD simulations have been tested in order to be able to reproduce realistic models of the polymer membranes. We have used the variation of surface to accessible volume (AV) ratio as well as its gradient, with the probe radius used to calculate the AV and surface of each amorphous cell, as a descriptor of the “goodness” of each packing at an intermediary stage of construction. After the elimination of the non-realistic boxes we have finally generated three realistic amorphous cells for each of the polymers. During the final amorphous cell generation the conformation and non-bonded pair interaction terms in the force field (torsion, non-bonded and coulomb interactions) have been first appropriately scaled down by 1:1000 followed by 1000 steps of conjugate gradient minimization and 1 ps of NPT dynamics and then the interactions were scaled up to original values in six steps (torsions in three steps 1:100, 1:10 and 1:1 with intermediary minimisation and NPT 1 ps relaxation followed by “non-bonded and coulomb” in three steps 1:100, 1:10 and 1:1 with intermediary minimisation and NPT 1 ps). Finally, a series of seven MD 5 ps compression runs [(NPT, 1 GPa, 300 K) (NVT, 600 K) (NVT, 300 K) (NPT, 0.1 GPa, 300 K) (NPT, 0.01 GPa, 300 K) (NPT, 0.001 GPa, 300 K) (NPT, 0.0001 GPa, 300 K, 30 ps)] followed by 300 ps NVT (300 K) have been performed for each amorphous cell to match the experimental density.

The permeation of small molecules through dense polymeric membranes occurs by the solution–diffusion mechanism involving two key steps [45,47–49]. In the first step, the penetrant molecules are dissolved and sorbed in the polymer matrix, while in the second one they diffuse through the medium. MD simulations are useful for calculating diffusion coefficients in rubbery polymers but do not sample large enough time scales to provide reliable information about glassy diffusion. The difficulties lie in the extremely broad distribution of gas molecule jump rates. It is known that the diffusion of a penetrant in a glassy polymer involves occasional jumps between cavities through the opening of a channel [12,15,50]. Jumps are rare events and the time between them is much shorter than the times governing matrix relaxation processes. For these reasons the diffusion coefficient can be estimated using transition-state theory (TST).

TST provides an approximate way to calculate the rate coefficient, k_{jump} , of each possible jump from cavity to cavity in a polymer microstructure. Gusev and Suter implemented the original TST method giving the polymer some flexibility [51,52] assuming that the polymer atoms,

in a sorption site, execute uncorrelated harmonic vibrations around their equilibrium positions to accommodate the guest molecules. The behaviour and properties of the small gas molecules can be described [53,54] with a time independent single-particle distribution function $\rho(r)$, where r is the position. The thermal fluctuations of the position of all atoms Δ are described by an isotropic Gaussian functional form. The smearing factor $\langle \Delta^2 \rangle$ is a parameter in the homogeneous isotropic approximation, which can be evaluated from atomistic trajectories of the polymeric matrix by means of short-scale MD simulations of the host matrix without dissolved molecules. The averaging time at which the smearing factor $\langle \Delta^2 \rangle$ is determined, should be the most frequent residence time τ of a probe molecule in the void. Since the value of the average time of penetrant molecules depends on the thermal vibrations of the polymer matrix an iterative procedure is used, starting with setting, rather arbitrarily, $\langle \Delta^2 \rangle = 0.3\text{--}0.4 \text{ \AA}$ and computing $\rho(\log \tau, \langle \Delta^2 \rangle)$.

2.1 Preparation of amorphous cell packings

The simulations of the amorphous cells of the membrane have been carried out using the InsightII (400P+) molecular modelling package of Accelrys and the COMPASS force field [44,53–55] going through the following steps:

1. Single repeat units of each of the four polymers have been constructed using the polymer BUILDER module of InsightII (400P+) molecular modelling package [43]. Charge groups have been assigned to fragments of each repeat unit and used for their energy minimisation employing a standard algorithm starting with a steepest-descent stage, switching to conjugate gradient when the energy derivative reaches $1000 \text{ kcal mol}^{-1} \text{ \AA}^{-1}$ followed by a Newton–Raphson optimisation algorithm. The final convergence criterion was to meet a derivative of $<0.001 \text{ kcal mol}^{-1} \text{ \AA}^{-1}$.
2. The isolated initial chain configurations of unsubstituted and alkylated PEEKs with a degree of polymerization of 100 have been constructed using the POLYMERISER module of InsightII (400P+) molecular modelling package. The backbone dihedral angle was set to random and the individual PEEK polymer chains were rapidly optimised (500 steps) using a group-based cut-off of 12 \AA with a spline-width of 1.0 \AA and a buffer-width of 0.5 \AA using a three stage minimization algorithm: steepest descents for initial relaxation (energy derivative $<1000 \text{ kcal mol}^{-1} \text{ \AA}^{-1}$) conjugate gradients (energy derivative $<10 \text{ kcal mol}^{-1} \text{ \AA}^{-1}$) and Newton–Raphson (energy derivative $<0.001 \text{ kcal mol}^{-1} \text{ \AA}^{-1}$). Each optimised chain was briefly relaxed through a 300 ps long molecular dynamics run with constant temperature (300 K) and time step of 1 fs. The Andersen method [56] was used to control the temperature. The relaxed chains were submitted again to optimisation following the three

stage protocol described above.

3. Bulk amorphous polymer structures have been generated using amorphous cell, which involves construction of chains in a periodic cell, at 303 K, with a RIS-based bond-by-bond construction method and taking account of bond torsion probabilities and bulk packing requirements [41,53]. To reduce the influence of chain ends on the simulations only a single long chain has been utilised. Several spacer molecules have been introduced in the amorphous cell to avoid the artefacts of catenated phenylene rings or a spearing of side groups or backbone chains through ring substructures as well as to confer realistic conformation to packed polymer chain. The spacers representing small obstacles (200 methanol molecules and three sets of 200 argon atoms) have been added sequentially in the simulation box before packing of the polymer. After a first relaxation using the basic-refine protocol of InsightII (400P+) employing an initial energy minimization followed by a NVT MD relaxation at 300 K and final energy minimisation the spacer molecules have been removed in the reverse order of their introduction in the box (first the 200 methanol molecules and then three sets of 200 argon atoms) followed by energy minimisation and MD relaxation–compression cycles after removal of each set.
4. The spacer-free packing models, with a reduced density in comparison to the experimental value, have been subjected to extensive equilibration procedures composed of sequences of energy minimization and NPT and NVT MD and annealing simulations combined with force field parameter (torsion, non-bonded and Coulomb interactions) scaling steps reported in table 1 associated with intermediary NVT and NPT MD relaxations as discussed above. The final equilibration stage is carried using a NVT run at 300 K for 300 ps duration time.
5. The goodness of each model has been analysed, before the complete equilibration procedure has been performed at an intermediate stage when the density of the packing boxes was at a value corresponding at the 90% of the experimental value. The variation of surface-to-volume ratio as well as its gradient with the probe radius has been used to analyse the AV

of each cell. The “Free Volume” routine implemented in Cerius2 simulation software [43] was used to calculate the AVs and surface areas using a probe sphere (with an adjustable radius) that is rolled through the amorphous periodic structure to generate a solvent accessible, internal void volume that has a corresponding internal surface area. Due to the size variation of probe molecules, the probe can only “see” a subset of the total free volume which is termed AV. The calculation method is very similar to connolly surface calculations and employs a grid method.

6. After this stage, by using with several cycles of NPT MD (constant particle number, temperature and pressure) runs at pressures of thousands of bars the density of the systems has been increased. Besides, simulated annealing runs with temperatures up to 1000 K and NVT dynamics at 303 K were used to further relax the polymer structure. The general simulation condition used were: minimum image boundary condition to make the system numerically tractable and to avoid symmetry effects; a cut-off distance of 15 Å with a switching function in the interval 13.5–15 Å. Through the dynamics, the Andersen [56] temperature control and the Berendsen [57] pressure control method have been used. The side length of the bulk models is of about 3 nm for all PEEKs.

2.2 Calculation of gas transport data in alkylated PEEK membranes

The TST after Gusev and Suter [41], as implemented in InsightII (400P+) [43], has been used to study the thermodynamics and transport of the small gas molecules, oxygen, nitrogen and carbon dioxide, respectively, in selected PEEKs packings. Diffusion coefficients (D) and gas solubility (S) in the matrix have been estimated, and the permeability coefficients (P) have been calculated by direct product of D and S . The calculation has been carried out in two steps. In the first step, the solubility (S) of the respective gas is evaluated. A 3D orthogonal lattice grid with a constant spacing of 0.3 Å has been used to estimate solute distribution function in the matrix by calculating the Helmholtz free energy between the gas molecule inserted at each grid point and all the atoms of the polymer matrix that are subject to elastic fluctuations. These data are used to identify minimum energetic sites and determine transition probabilities from site to site together with the residence times in each site.

In the second step a Monte Carlo simulation of gas diffusion by a “hopping” mechanism has been performed based on the energy as well as connectivity of sites and the transition jump probabilities. In this study, the smearing factor has been computed using the self-consistent field (SCF) procedure. The mean square displacement (MSD) of all subsets of atoms in the amorphous cell is obtained as a function of time from a short NVT dynamics (30 ps with 1 fs time step at 300 K).

Table 1. Scaling procedure of FF energy terms torsion, non-bonded and coulomb interactions.

Stage of equilibration	Scaling factor for the conformation energy terms in the force field	Type of non-bonded interaction energy terms (EvdW)	Type of non-bonded interaction energy terms (ECoulomb)
1	0.001	0.001	0.001
2	0.01	0.001	0.001
3	0.1	0.001	0.001
4	1	0.001	0.001
5	1	0.01	0.01
6	1	0.1	0.1
7	1	1	1

Table 2. Free volume analysis of generated amorphous cells using a 1.7 Å probe.

Polymer	Amorphous cells	Density (g/cm ³)	Accessible volume (Å ³)/cell	Surface/accessible volume ratio	$D(O_2)$ (cm ³ /s) × 10 ⁻⁶	$S(O_2)$ (cm ³ (STP)/cm ³ Pa) × 10 ⁻⁵
PEEKWC	Cell_1	1.173	1332.31	1.63	1.81	2.11
	Cell_2	1.179	1725.15	1.38	3.03	2.01
	Cell_3	1.181	1684.58	1.59	3.85	1.95
DMPEEK	Cell_1	1.394	791.81	1.47	1.60	1.89
	Cell_2	1.041	4960.52	0.89	1.13	1.75
	Cell_3	1.081	2668.84	1.38	6.88	2.03
TMPEEK	Cell_1	1.131	1332.31	1.63	1.81	2.11
	Cell_2	1.094	1725.15	1.38	3.03	2.01
	Cell_3	1.095	1684.58	1.59	3.85	1.95
DIDMPEEK	Cell_1	1.063	1652.71	1.57	2.05	1.94
	Cell_2	1.042	2451.20	1.54	4.28	1.98
	Cell_3	1.041	2716.77	1.32	3.27	2.01

3. Results and discussion

The protocol that we have used in this study for generating the models of the PEEKs membranes combined with the intermediary control of free volume distribution in the matrix have increased the reproducibility model cells construction. This has been validated by the TST simulations, which show reduced differences between predicted S and D values of the same gas in different model cells of the same polymer. In the following we report results of the performed calculations.

3.1 Construction of realistic amorphous models

It has been clearly shown in the literature [12,15,21,22,24,30] that the transport properties of small gases through glassy polymer membranes are strongly controlled by the free volume and its distribution. For this reason the amorphous cells models of the PEEKs have been generated using a single polymer chain only, in order to minimize chain end effects, which would lead to increased density of chain ends and consequently would imply an increased free volume. In this study, we have further “optimised” the idea of solvent inclusion in generating the amorphous cells. Before starting the packing of the polymer chain in the cell we insert 200 methanol molecules as well as three time 200 argon atoms. This allows a much more “homogeneous” packed chain configuration as well as a more uniform free volume distribution within the matrix. The reason why the solvent has been introduced is that it can be removed in several stages while compressing the cell in order to increase the density. The “solvent insertion” step reduces considerably the probability of finding catenated phenylene rings or a spearing of side groups or backbone chains through ring sub-structures.

After each step of solvent removal, several cycles of an initial energy minimization followed by a brief NVT run at 303 K and then a final energy minimization has been performed. After the removal of the last set of argon atoms and the carrying out of the NVT dynamics, followed by the energy minimisation, the density of the generated cells corresponded to nearly 90% of the experimental value.

In table 2 we report the calculated data for 12 PEEKs cells using a probe with a radius of 1.7 Å (that correspond to the kinetic diameter of oxygen molecule). The accessible surface area (ASA) and AV were calculated with the free volume utility of the visualizer module of the Cerius2 4.2 software package [58] using the “Accessible” mode together with the “Fine” grid spacing specifications. A spherical probe atom with a defined radius R is rolled inside the amorphous cell polymer packing generating a diffusion-accessible surface. The AV for a probe of radius R is defined as volume in the polymer matrix traced out by the probe’s centre for all the regions in which the probe can fit. The occupiable volume is just the AV for a penetrant with radius $R = 0$ Å. By varying the probe radius it is possible to generate a series of ASA and AV values for each polymer packing and using an in-house MATLAB program to tabulate and plot the variation of ASA to AV ratio as well as its gradient. The calculations have been repeated systematically by varying the probe radius in the interval between 1.2 and 2.1 Å, with a 0.1 Å as step. The analysis of the obtained data allowed us to establish a correlation between the variation of the ratio between accessible surface and AV, as well as its gradient, with the pore radius and the goodness of the cells. We report in figure 2 the variation of these quantities for the three generated models of DMPEEK. On the basis of their variations we have excluded the cell_2 of this polymer from our further simulation. We have thus generated a new cell in order to have three final membrane structures for each of polymers.

The successive step, besides the check on the quality of boxes at an intermediate stage, has been the reaching of the experimental density by increasing the pressure with several cycles of NPT MD (constant particle number, temperature and pressure) runs at pressures of thousands of bars. Moreover, simulated annealing runs with temperatures up to 1000 K and NVT dynamics at 303 K have been used to further relax the polymeric structures. Equilibration and density adjustment of the polymer system have been achieved through a final 300 ps MD run.

It is worth to say that small deviations in obtaining the experimental density may happen for glassy stiff-chain

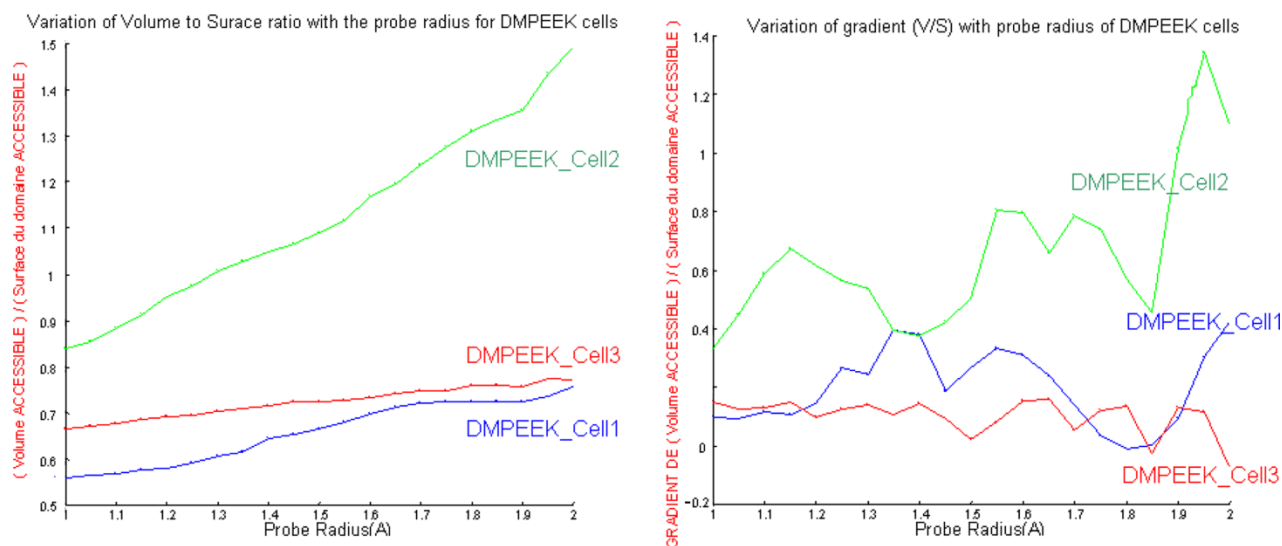


Figure 2. Variation of volume to surface ratio and its gradient with probe radius.

polymer materials [10,15,40] particularly if the models are rather large. The deviations may reflect minor errors of the parameterization of the respective polymers in the chosen force field, which influence the equilibration of the models. In table 3 we report the free volume analysis results for the equilibrated membrane model membrane packings using a probe with 1.7 Å.

3.2 TST prediction of gas transport properties

The equilibrated amorphous cells are used in the TST calculations for estimating the solubilities and diffusion coefficients for O₂, N₂ and CO₂ molecules for each cell. It is to notice that the TST calculations using the gsdiff/gsnet software code [59,60] assume that the penetrant molecules are spherical united atoms characterised by effective Lennard–Jones parameters (σ, ϵ) expressed in (Angstroms, kcal/mol). In all the calculations we have used the default values of these parameters O₂ (3.460, 0.2344), N₂ (3.698, 0.1889) and CO₂ (4.000, 0.4500). In tables 4 and 5 are reported, respectively, the results of TST simulations and experimental measurements for O₂, N₂ and CO₂ molecules for the 12 equilibrated amorphous cells of the selected PEEKs. The interaction energy between each gas molecule and the polymer matrix is calculated on all node positions of the fine grid layered over the amorphous polymer packing cells. It is to notice that only the Van der Waals (Lennard–Jones potentials) interactions are considered. Furthermore, it is assumed that the polymer packing does not have to undergo structural relaxation (e.g. resulting from torsion transitions) to accommodate an inserted particle. Therefore, this simulation technique is restricted to small molecules. From, table 4 it appears clear that the simulated values are more self-consistent showing less scatter than in recently reported papers dealing with modeling of alkylated PEEK membranes [14,39,40] confirming in this way the new simulation protocol for generating realistic

amorphous cells models of these membranes. An inspection of reported values in tables 4 and 5 indicates that a relatively good agreement is obtained for O₂ and N₂ molecules and important deviations between simulated and experimental values are observed for CO₂ for diffusion coefficient as well as the solubility. It is important to notice that if one compares only the permeabilities, due to an error compensation for the CO₂, would come to the conclusion that its transport properties through alkylated PEEK membranes are better represented than those of O₂ and N₂. In order to analyse the discrepancies between experimental and simulated results we report in table 6 the ratio of simulated to experimental values of D and S at 300 K for N₂, O₂ and CO₂ molecules for the 12 generated cells together with a comparison of simulated to experimental ideal separation factors α_{O_2, N_2} and α_{N_2, CO_2} . The reported experimental to simulated D ratio values indicate that the TST simulated results for N₂ and O₂ are overestimated by a factor varying between 1.1 and 9.1 with respective (mean, standard deviation) for O₂ (4.1, 2.3) and N₂ (4.2, 2.7). On the contrary the TST simulated results for CO₂ are underestimated by a factor varying between 8.7 and 67.2. The tabulated experimental to simulated S ratio values show the TST simulated results for N₂ and O₂ overestimated by a factor varying between 2.3 and 4.7 (mean, standard deviation), respectively, for O₂ (3.97, 0.52) and N₂ (3.08, 0.54). The TST simulated results for CO₂ are also overestimated by a factor varying between 4.6 and 17.3 with mean, standard deviation of 10.5, 4.7, respectively.

The large deviations for CO₂ might be explained by the well known experimental fact of plasticisation of glassy membranes due to specific interactions of CO₂ with the polymer matrix leading to membrane structural relaxations. This behavior “violates” the assumption of the TST in which the dynamics of the dissolved molecules is coupled only to the elastic thermal motion of the dense polymer. The results for CO₂ show clearly the necessity

Table 3. Free volume analysis results for equilibrated cells using a 1.7 Å probe.

Model		Free volume with probe radius of 1.7 Å							
Polymer	Density (g/cm ³)	Available volume (Å ³)	Occupiable volume (Å ³)	Accessible volume (Å ³)	Surface area	FFV	Fractional occupiable volume (%)	Fractional accessible (%)	S(Acc) / V(Acc)
PEEKWC	1.25	18146.2	194.6	93.5	146.4	0.083	0.328	0.158	1.565
	1.25	18169.9	236.9	101.0	135.4	0.084	0.399	0.179	1.341
	1.25	18142.4	192.4	111.9	160.3	0.083	0.324	0.189	1.433
DMPEEK	1.247	18659.9	267.5	145.0	203.9	0.072	0.425	0.231	1.406
	1.247	18583.4	240.7	79.7	126.5	0.070	0.383	0.127	1.587
	1.247	18644.9	284.7	136.6	215.9	0.071	0.453	0.217	1.581
TMPEEK	1.195	21688.1	328.3	105.3	152.3	0.094	0.475	0.152	1.447
	1.195	21681.7	285.6	127.7	197.9	0.094	0.413	0.185	1.550
	1.195	21696.1	281.0	89.4	132.1	0.094	0.407	0.129	1.478
DIDMPEEK	1.14	25805.5	501.6	121.0	181.3	0.107	0.629	0.152	1.498
	1.14	25856.0	525.9	214.8	319.8	0.108	0.659	0.269	1.489
	1.14	25837.6	471.6	201.8	307.8	0.107	0.591	0.253	1.525

Table 4. TST predicted *S* and *D* values of O₂, N₂ and CO₂ in selected PEEKs.

Model		TST								
Polymer	Density (g/cm ³)	O ₂			N ₂			CO ₂		
		<i>D</i> (cm ² /s) × 10 ⁻⁸	<i>S</i> (cm ³ (STP)/cm ³ Pa) × 10 ⁻⁵	Permeability (barrer)	<i>D</i> (cm ² /s) × 10 ⁻⁸	<i>S</i> (cm ³ (STP)/cm ³ Pa) × 10 ⁻⁵	Permeability (barrer)	<i>D</i> (cm ² /s) × 10 ⁻⁸	<i>S</i> (cm ³ (STP)/cm ³ Pa) × 10 ⁻⁵	Permeability (barrer)
PPEEKWC	1.25	4.7	1.47	9.25	1.1	0.87	1.33	0.017	48.20	1.10
	1.25	4.0	1.45	7.63	0.8	0.86	0.97	0.016	39.80	0.83
	1.25	2.8	1.23	4.51	0.7	0.70	0.63	0.011	30.80	0.46
DDMPEEK	1.247	8.5	1.50	16.98	1.3	0.89	1.56	0.037	39.00	1.90
	1.247	12.7	1.23	20.89	2.1	0.74	2.02	0.052	31.80	2.19
	1.247	7.6	1.60	16.29	1.1	0.97	1.43	0.024	44.55	1.44
TTMPEEK	1.195	22.2	1.61	47.74	3.6	0.91	4.29	0.071	36.10	3.42
	1.195	23.2	1.26	39.00	3.6	0.69	3.33	0.122	22.80	3.71
	1.195	26.4	1.45	50.97	4.6	0.77	4.75	0.140	26.51	4.94
DIDMPEEK	1.14	15.7	1.45	30.40	4.0	0.84	4.51	0.1	27.20	3.41
	1.14	26.8	1.52	50.79	6.9	0.81	7.43	0.209	23.20	6.52
	1.14	30.4	1.26	51.11	7.8	0.74	7.67	0.223	24.00	7.13

Table 5. Experimental values of transport properties of O₂, N₂ and CO₂ in selected PEEKs.

Model		Experimental data								
Polymer	Density (g/cm ³)	O ₂			N ₂			CO ₂		
		Diffusion (cm ² /s) × 10 ⁻⁸	Solubility (cm ³ (STP)/cm ³ Pa) × 10 ⁻⁵	Permeability (barrer)	Diffusion (cm ² /s) × 10 ⁻⁸	Solubility (cm ³ (STP)/cm ³ Pa) × 10 ⁻⁵	Permeability (barrer)	Diffusion (cm ² /s) × 10 ⁻⁸	Solubility (cm ³ (STP)/cm ³ Pa) × 10 ⁻⁵	Permeability (barrer)
PPEEKWC	1.25	2.15	0.343	9.25	0.618	0.243	0.193	0.746	2.835	2.73
DDMPEEK	1.247	1.96	0.344	0.87	0.295	0.251	0.095	0.639	3.151	2.6
TTMPEEK	1.195	3.31	0.363	1.55	0.516	0.281	0.187	1.22	3.467	5.44
DIDMPEEK	1.14	9.12	0.413	4.85	2.25	0.322	0.936	3.83	5.129	19.3

Table 6. Comparison of the ratio of experimental to simulated *D*, *S* for O₂, N₂ and CO₂ together with separation factors α_{O₂,N₂} and α_{N₂,CO₂} in selected PEEKs.

Polymer	Model.car./arc	<i>D</i> _{(Exp)/<i>D</i>_(Calc)}			<i>S</i> _{(Exp)/<i>S</i>_(Calc)}			Experimental		Calculated	
		O ₂	N ₂	CO ₂	O ₂	N ₂	CO ₂	<i>P</i> _{(O₂)/<i>P</i>_(N₂)}	<i>P</i> _{(CO₂)/<i>P</i>_(N₂)}	<i>P</i> _{(O₂)/<i>P</i>_(N₂)}	<i>P</i> _{(CO₂)/<i>P</i>_(N₂)}
PEEKWC	cell_1	0.46	0.54	43.6	0.23	0.27	0.058	4.92	2.87	6.97	0.12
	cell_2	0.54	0.73	47.8	0.23	0.28	0.071	4.92	2.87	7.84	0.11
	cell_3	0.78	0.90	67.2	0.27	0.34	0.058	4.92	2.87	7.12	0.10
DMPEEK	Cell_1	0.23	0.23	17.5	0.22	0.28	0.079	9.16	3.98	10.91	0.11
	Cell_2	0.15	0.14	12.4	0.27	0.33	0.097	9.16	3.98	10.34	0.10
	Cell_3	0.26	0.27	26.4	0.21	0.25	0.069	9.16	3.98	11.39	0.09
TMPEEK	Cell_1	0.15	0.15	17.2	0.22	0.30	0.094	8.29	3.51	11.12	0.07
	Cell_2	0.14	0.14	10.0	0.28	0.40	0.149	8.29	3.51	11.70	0.10
	Cell_3	0.13	0.11	8.7	0.25	0.36	0.128	8.29	3.51	10.74	0.10
DIDMPEEK	Cell_1	0.58	0.56	40.7	0.28	0.37	0.185	5.18	3.98	6.75	0.11
	Cell_2	0.34	0.33	18.3	0.29	0.39	0.215	5.18	3.98	6.84	0.13
	Cell_3	0.30	0.29	17.2	0.32	0.43	0.210	5.18	3.98	6.66	0.14

Table 7. Comparison of predicted to experimental diffusion selectivities and solubility selectivities for (O₂, N₂) and (N₂, CO₂) in selected PEEKs.

Polymer	Model.cell/arc	$D_{(selectivity)}$				$S_{(selectivity)}$			
		Exp (O ₂ /N ₂)	Sim (O ₂ /N ₂)	Exp (CO ₂ /N ₂)	Sim (CO ₂ /N ₂)	Exp (O ₂ /N ₂)	Sim (O ₂ /N ₂)	Exp (CO ₂ /N ₂)	Sim (CO ₂ /N ₂)
PEEKWC	Cell_1	4.05	4.3	1.70	0.020	1.28	1.69	15.92	55.40
	Cell_2	4.05	5.0	1.70	0.019	1.28	1.69	15.92	46.28
	Cell_3	4.05	4.0	1.70	0.016	1.28	1.76	15.92	44.00
DMPEEK	cell_1	6.64	6.5	2.17	0.042	1.37	1.69	12.56	43.82
	cell_2	6.64	6.0	2.17	0.070	1.37	1.66	12.56	42.97
	cell_3	6.64	6.9	2.17	0.025	1.37	1.65	12.56	45.93
TMPEEK	cell_1	6.41	6.2	2.36	0.078	1.29	1.77	12.32	39.67
	cell_2	6.41	6.4	2.36	0.177	1.29	1.83	12.32	33.04
	cell_3	6.41	5.7	2.36	0.182	1.29	1.88	12.32	34.43
DIDMPEEK	cell_1	3.48	3.9	1.21	0.119	1.41	1.73	11.68	32.38
	cell_2	3.48	3.9	1.21	0.258	1.41	1.88	11.68	28.64
	cell_3	3.48	3.9	1.21	0.301	1.41	1.70	11.68	32.43

to develop improved TST-methods which permit the matrix to be locally flexible in order to accommodate larger penetrant molecules that are described in all-atom with partial charges representation. A better agreement between simulated and experimental D and S for N₂ and O₂ could be easily obtained by reparametrisation of Lennard–Jones parameters of the both gas molecules but this was not the objective of this study.

In table 7 the comparison of predicted to experimental diffusion and solubility selectivities reinforces the conclusions obtained from the analysis of table 6. The predicted diffusion selectivity [$\alpha(D)_{O_2,N_2}$] nicely reproduces the experimentally observed trend for O₂ and N₂ diffusion while the predicted [$\alpha(D)_{CO_2,N_2}$] it is more than one order of magnitude off the experimental values. The predicted trend for solubility selectivity for O₂ and N₂ [$\alpha(S)_{O_2,N_2}$] is in perfect agreement with the experimental observation with a slightly higher estimation of relative O₂ solubility. The predicted solubility selectivity for CO₂ and N₂ [$\alpha(S)_{CO_2,N_2}$] is more than three times higher than the experimental one.

4. Conclusions

A new protocol for packing glassy polymer with intermediate control of free volume distribution has been applied for four alkylated PEEKs, namely DMPEEK, TMPEEK and DIDMPEEK. The TST approach of Gusev–Suter methodology was used to calculate diffusion and solubility coefficients for N₂, O₂ and CO₂ gas molecules in the generated membrane models. The comparison of modelled values of modified PEEK-WC with the experimental ones indicates that the new approach of packing produces amorphous cells that show less scatter in predicted S and D values with respect to recent published papers dealing with these membranes [14,39,40]. A better agreement between simulated and experimental permeabilities could be obtained for improving prediction of absolute gas transport properties in glassy polymer membranes by re-parametrisation of

Lennard–Jones parameters of the penetrant gas molecules.

Acknowledgements

The work was in part supported by the European Commission 6th Framework Program Project MULTIM-ATDESIGN “Computer aided molecular design of multifunctional materials with controlled permeability properties” Contract Number: NMP3-CT-2005-013644”.

References

- [1] P.V.K. Pant, R.H. Boyd. Simulation of diffusion of small penetrants in polymers. *Macromolecules*, **114**, 494 (1992).
- [2] P.V.K. Pant, R.H. Boyd. Molecular-dynamics simulation of diffusion of small penetrants in polymers. *Macromolecules*, **26**, 679 (1993).
- [3] F. Müller-Plathe. Permeation of polymers—a computational approach. *Acta Polym.*, **45**, 259 (1994).
- [4] A.A. Gusev, F. Müller-Plathe, W.F. Van Gunsteren, U.W. Suter. Dynamics of small molecules in bulk polymers. *Adv. Polym. Sci.*, **116**, 207 (1994).
- [5] P.V.K. Pant, D.N. Theodorou. A strategy for atomistic Monte Carlo simulation of polydisperse polymer systems. *Polym. Prepr. (Am. Chem. Soc. Div. Polym. Chem.)*, **35**, 165 (1994).
- [6] D. Hofmann, J. Ulbricht, D. Fritsch, D. Paul. Molecular modelling simulation of gas transport in amorphous polyimide and poly(amide imide) membrane materials. *Polymer*, **37**, 4773 (1996).
- [7] H. Takeuchi, K. Okazaki. Dynamics of small molecules in a dense polymer matrix: molecular dynamics studies. *Mol. Simul.*, **16**, 59 (1996).
- [8] J.R. Fried, D.K. Goyal. Molecular simulation of gas transport in poly[1-(trimethylsilyl)-1-propyne]. *J. Polym. Sci. Part B: Polym. Phys.*, **36**, 519 (1998).
- [9] R.K. Bharadwaj, R.H. Boyd. Small molecule penetrant diffusion in aromatic polyesters: a molecular dynamics simulation study. *Polymer*, **40**, 4229 (1999).
- [10] D. Hofmann, L. Fritz, J. Ulbricht, C. Schepers, M. Bohning. Detailed-atomistic molecular modeling of small molecule diffusion and solution processes in polymeric membrane materials. *Macromol. Theory Simul.*, **9**, 293 (2000).
- [11] M. Lopez-Gonzalez, E. Saiz, J. Guzman, E. Riande. Experimental and simulation studies on the transport of gaseous diatomic molecules in polycarbonate membranes. *J. Chem. Phys.*, **115**, 6728 (2001).
- [12] F. Müller-Plathe. Molecular simulation of polymers: from concepts to industrial applications. *DECHEMA Monographien*, **137**, 163 (2001).

- [13] R. Shanks, D. Pavel. Simulation of diffusion of O₂ and CO₂ in amorphous poly(ethylene terephthalate) and related alkylene and isomeric polyesters. *Mol. Simul.*, **28**, 939 (2002).
- [14] E. Tocci, E. Bellacchio, N. Russo, E. Drioli. Diffusion of gases in PEEKs membranes: molecular dynamics simulations. *J. Membr. Sci.*, **206**, 389 (2002).
- [15] M. Heuchel, D. Hofmann, P. Pullumbi. Molecular modeling of small molecule permeation in polyimides and its correlation to free volume distributions. *Macromolecules*, **37**(1), 201 (2004).
- [16] N.C. Karayiannis, V.G. Mavrantzas, D.N. Theodorou. Detailed atomistic simulation of the segmental dynamics and barrier properties of amorphous poly(ethylene terephthalate) and poly(ethylene isophthalate). *Macromolecules*, **37**, 2978 (2004).
- [17] S. Neyertz, D. Brown. Influence of system size in molecular dynamics simulations of gas permeation in glassy polymers. *Macromolecules*, **37**, 10109 (2004).
- [18] V.E. Raptis, I.G. Economou, D.N. Theodorou, J. Petrou, J.H. Petropoulos. Molecular dynamics simulation of structure and thermodynamic properties of poly(dimethylsilamethylene) and hydrocarbon solubility therein: toward the development of novel membrane materials for hydrocarbon separation. *Macromolecules*, **37**, 1102 (2004).
- [19] D. Hofmann, M. Entrialgo-Castano, A. Lerbret, M. Heuchel, Y. Yampolskii. Molecular modeling investigation of free volume distributions in stiff chain polymers with conventional and ultrahigh free volume: comparison between molecular modeling and positron lifetime studies. *Macromolecules*, **36**, 8528 (2003).
- [20] D. Hofmann, M. Heuchel, Y. Yampolskii, V. Khotimskii, V. Shantarovich. Free volume distributions in ultrahigh and lower free volume polymers: comparison between molecular modeling and PALS studies. *Macromolecules*, **35**, 2129 (2002).
- [21] B.D. Freeman. Basis of permeability/selectivity tradeoff relations in polymeric gas separation membrane. *Am. Chem. Soc.*, **32**, 375 (1999).
- [22] S.A. Stern, W.J. Koros. Separation of gas mixtures with polymer membranes a brief overview. *Chim. Nouv.*, **18**, 3201 (2000).
- [23] L.M. Robeson, W.F. Burgoyne, M. Langsam, A.C. Savoca, C.F. Tien. High performance polymers for membrane separation. *Polymer*, **35**, 4970 (1994).
- [24] L.M. Robeson. Structure/property studies on polymeric materials. Abstracts of Papers, 225th ACS National Meeting, New Orleans, LA, United States, March 23–27 (2003).
- [25] L.M. Robeson, W.F. Burgoyne, M. Langsam, A.C. Savoca, C.F. Tien. High performance polymers for membrane separation. *Polymer*, **35**, 4970 (1994).
- [26] S.A. Stern. Polymers for gas separations: the next decade. *J. Membr. Sci.*, **94**, 1 (1994).
- [27] C.M. Zimmerman, A. Singh, W.J. Koros. Tailoring mixed matrix composite membranes for gas separations. *J. Membr. Sci.*, **137**, 145 (1997).
- [28] W.J. Koros, G.K. Fleming. Membrane-based gas separation. *J. Membr. Sci.*, **83**, 1 (1993).
- [29] L.M. Robeson. *Correlation of Separation Factor versus Permeability for Polymeric Membranes*, p. 165, Elsevier Science Publishers, Amsterdam (1991).
- [30] W.J. Koros, M.R. Coleman, D.R.B. Walker. Controlled permeability polymer membranes. *Annu. Rev. Mater.*, **22**, 47 (1992).
- [31] I.C. Roman, R.W. Ubersax, G.K. Fleming. *New Directions in Membranes for Gas Separation in Chimica e l'Industria*, Milan, Italy, 83, pp. e1/1 (2001).
- [32] D.R. Paul, M.R. Pixon. Polyarylate gas separation membranes. *Macromol. Symp.*, **118**, 401 (1997).
- [33] H.C. Zhang, T.L. Chen, Y.G. Yuan. Synthesis of new type polyether ether ketone with phtalein lateral group. Chinese Patent (1987).
- [34] K. Liu, H.C. Zhang, T.L. Chen, Y.G. Yuan. Single-step process for synthesizing polyarylethersulfones with peptide side chain. Chinese Patent (1986).
- [35] F. Lufrano, E. Drioli, G. Golemme, L. Di Giorgio. Transport parameters of carbon dioxide in PEEK membr. *J. Membr. Sci.*, **113**, 121 (1996).
- [36] M.G. Buonomenna, A. Figoli, J.C. Jansen, E. Drioli. Preparation of asymmetric PEEKWC flat membranes with different microstructures by wet phase inversion. *J. Appl. Polym. Sci.*, **92**, 576 (2004).
- [37] F. Tasselli, J.C. Jansen, E. Drioli. PEEKWC ultrafiltration hollow-fiber membranes: preparation, morphology, and transport properties. *J. Appl. Polym. Sci.*, **91**, 841 (2004).
- [38] J.C. Jansen, M. Macchione, E. Drioli. High flux asymmetric gas separation membranes of modified poly(ether ether ketone) prepared by the dry phase inversion technique. *J. Membr. Sci.*, **255**, 167 (2005).
- [39] E. Tocci, M.P. Perrone, N. Russo, E. Drioli. Molecular simulations of gas transport properties of alkylated PEEK membrane. *J. Mol. Graph. Model.*, in press (2005).
- [40] E. Tocci, D. Hofmann, D. Paul, N. Russo, E. Drioli. A molecular simulation study on gas diffusion in a dense poly(ether-ether-ketone) membr. *Polymer*, **42**, 521 (2001).
- [41] D.N. Theodorou, U.W. Suter. Detailed molecular structure of a vinyl polymer glass. *Macromolecules*, **18**, 1467 (1985).
- [42] Z. Wang, T. Chen, J. Xu. Gas transport properties of novel cardo poly(aryl ether ketone)s with pendant alkyl groups. *Macromolecules*, **33**, 5672 (2000).
- [43] I. Accelrys. Accelrys, Inc. San Diego, CA, USA. [InsightII(400P+) software package] (2004).
- [44] D. Rigby, H. Sun, B.E. Eichinger. Computer simulations of Poly(ethylene oxide): FF, PVT diagram and cyclization behavior. *Polym. Int.*, **44**, 311 (1997).
- [45] J. Bicerano. *Prediction of Polymer Properties*, 2nd ed., Marcel Dekker, New York (1996).
- [46] H.J. Meriovitch. Computer simulation of self-avoiding walks: testing the scanning method. *J. Chem. Phys.*, **79**, 502 (1983).
- [47] W.J. Koros, G.K. Fleming. Membrane-based gas separation. *J. Membr. Sci.*, **83**, 1 (1993).
- [48] R.M. Sok, H.J.C. Berendsen, W.F. van Gunsteren. Molecular dynamics simulation of the transport of small molecules across a polymer membrane. *J. Chem. Phys.*, **96**, 4699 (1992).
- [49] S.A. Stern. Polymers for gas separations: the next decade. *J. Membr. Sci.*, **94**, 1 (1994).
- [50] N.F.A. Van der Vegt. Temperature dependence of gas transport in polymer melts: molecular dynamics simulations of CO₂ in polyethylene. *Macromolecules*, **33**, 3153 (2000).
- [51] A.A. Gusev, U.W. Suter. Dynamics of small molecules in dense polymers subject to thermal motion. *J. Chem. Phys.*, **99**, 2228 (1993).
- [52] A.A. Gusev, S. Arizzi, U.W. Suter. Dynamics of light gases in rigid matrices of dense polymers. *J. Chem. Phys.*, **99**, 2221 (1993).
- [53] D.N. Theodorou, U.W. Suter. Atomistic modeling of mechanical properties of polymeric glasses. *Macromolecules*, **19**, 139 (1986).
- [54] I. Accelrys. Accelrys, Inc. San Diego, CA, USA. [InsightII(400P+) software package] Polymer User Guide. Polymerizer section (2004).
- [55] H. Sun, D. Rigby. Polysiloxanes: *Ab Initio* force field and structural, conformational and thermophysical properties. *Spectrochim. Acta A*, **153**, 1301 (1997).
- [56] T.A. Andrea, W.C. Swope, H.C. Andersen. The role of long ranged forces in determining the structure and properties of liquid water. *J. Chem. Phys.*, **79**, 4576 (1983).
- [57] H.J.C. Berendsen, J.P.M. Postma, W.F. Van Gunsteren, A. DiNola, J.R. Haak. Molecular dynamics with coupling to an external bath. *J. Chem. Phys.*, **81**, 3684 (1984).
- [58] I. Accelrys. Accelrys, Inc. San Diego, CA, USA. [Ceri2 software package] (2004).
- [59] I. Accelrys. Implemented as gsnet/gsdiff in InsightII(400P+) Accelrys, Inc (2000).
- [60] A. Tiller. Implemented as gsnet/gsdiff code in InsightII (400P+) molecular modeling software package. Accelrys, Inc (1993).